


Evaluation of a mobile C-arm cone-beam CT in interstitial high-dose-rate prostate brachytherapy treatment planning

Mario Djukelic, MPhys, MEd,^{1,2}  David Waterhouse, PhD,³ Ryan Toh, BSc,³ Hendrick Tan, MBBS,³ Pejman Rowshanfarzad, PhD,² David Joseph, MBBS, FRANZCR,³ & Martin A. Ebert, PhD^{2,3}

¹Department of Medical Technology and Physics, Sir Charles Gairdner Hospital, Nedlands, WA, Australia

²Department of Physics, The University of Western Australia, Crawley, WA, Australia

³Department of Radiation Oncology, Sir Charles Gairdner Hospital, Nedlands, WA, Australia

Keywords

C-arm CT, cone-beam CT, high-dose-rate brachytherapy, interstitial brachytherapy, prostate cancer

Correspondence

Mario Djukelic, Department of Medical Technology and Physics, Level G, G Block, Sir Charles Gairdner Hospital, Hospital Avenue, Nedlands, 6009 Western Australia, Australia.
Tel: +61 8 6457 2866;
E-mail: mario.djukelic@health.wa.gov.au

Received: 17 September 2018; Revised: 25 February 2019; Accepted: 28 February 2019

J Med Radiat Sci **66** (2019) 112–121

doi: 10.1002/jmrs.331

Abstract

Introduction: The aim of this study was to evaluate the suitability of using cone-beam computed tomography (CBCT) obtained with a mobile C-arm X-ray fluoroscopy unit as a single modality for planning of high-dose-rate (HDR) prostate brachytherapy treatments. **Methods:** The feasibility of using CBCT images obtained using a Siemens Arcadis Orbic 3D mobile C-arm was evaluated. A retrospective clinical study was undertaken of six participants undergoing HDR prostate brachytherapy. Plans generated using images from a Toshiba Aquilion One LB CT were compared with those generated using CBCT images. After rigid spatial registration, the plans were compared based on various parameters such as dose-volume histograms, overlap quantities and metrics, and dose constraints. **Results:** Provided they were within the limited field of view, the brachytherapy catheters and fiducial markers were clearly visible in the CBCT images and thus, localisable and identifiable in the treatment planning process. The Siemens CBCT underestimated CT numbers leading to poorer tissue contrast which exacerbated the difficulties in delineation of the target tumour and the surrounding organs at risk. Between CT- and CBCT-based plans, the mean difference of CTV- D_{90} was 1.58 Gy, CTV- V_{100} was 12.13%, rectum- V_{80} was 0.06% and urethra- V_{120} was -0.70%. **Conclusion:** It was not feasible to solely utilise the Siemens Arcadis Orbic 3D for HDR prostate brachytherapy treatment planning due to suboptimal organ delineation. However, the methods in this study could be used to evaluate other mobile CBCT imaging devices for feasibility in HDR brachytherapy treatment planning since the results indicated that it may not be necessary to have standard quality CT images for treatment planning.

Introduction

Interstitial high-dose-rate (HDR) brachytherapy is a form of prostate radiotherapy. Most commonly, HDR prostate brachytherapy involves the transperineal insertion of 15–20 hollow steel, titanium or plastic needles (brachytherapy afterloading catheters) along with fiducial markers into the prostate. The radioactive source is successively pushed by an automatic afterloader, and left to dwell at a number of predefined positions within the catheters. Depending on availability at the clinical centre, computed tomography (CT), magnetic resonance imaging

(MRI) or transrectal ultrasound (TRUS) are utilised to acquire images of the prostate and pelvis for treatment planning, which requires identification of the catheters and fiducial markers, as well as delineation of the clinical target volume (CTV) and the organs at risk (OAR).

Cone-beam CT (CBCT) scanners are becoming more available in surgical theatres and are commonly used in image guidance in radiotherapy, angiography, mammography and orthopaedics.¹ Previous studies^{2–6} have investigated CBCT in the context of brachytherapy. Al-Halabi et al.² utilised CBCT for intracavitary HDR brachytherapy treatment planning for cervical cancer and

were able to sufficiently delineate the CTV and OARs (bladder and rectum). Holly *et al.*³ used CBCT to study catheter displacement between time of planning and time of treatment delivery for patients having HDR prostate brachytherapy. It was demonstrated that catheter displacement frequently occurs and affects dose distributions. This issue could be solved by readjusting the catheters. Herrmann *et al.*⁴ studied the displacement of fiducial gold markers due to needle insertion in HDR brachytherapy for prostate cancer. Marker displacement was evident and they successfully localised and adjusted the marker position by means of CBCT. Batchelar *et al.*⁵ compared the accuracy of catheter localisation in HDR brachytherapy for prostate cancer between TRUS and CBCT. The group concluded that the use of ultrasound for needle tip localisation was at least as accurate as cone-beam CT. Even *et al.*⁶ utilised TRUS for organ delineation and CBCT for needle identification in HDR brachytherapy for prostate cancer. They concluded that the method was accurate and clinically useful.

Using a mobile C-arm CBCT scanner over a CT for HDR prostate brachytherapy treatment planning has potential advantages. The mobility of the scanner allows scanning the pelvis immediately after surgery giving direct indication of the catheter locations. Any patient movement provides an opportunity for the implant to move relative to the anatomy. The mobile CBCT scanner makes the patient movement to and from the CT room redundant which enhances patient comfort and saves time. The mobility of the C-arm CBCT has the potential to improve the workflow, reduce overall treatment time, lower capital and maintenance costs, and increase the availability of CT scanners for other patients.

This report describes an assessment of a mobile C-arm CBCT scanner, the Siemens Arcadis Orbic 3D (Siemens Healthineers, Erlangen, Germany), for generating CT images for HDR prostate brachytherapy treatment planning. Following generic image quality assessments, an ethics approved clinical study was conducted where treatment plans were created based on both the Siemens CBCT and CT images (Toshiba Aquilion LB, Toshiba Medical, Otawara, Japan) for patients undergoing HDR prostate brachytherapy, and assessed them for qualitative and quantitative differences.

Methods and Materials

Image quality assessment

Spatial resolution and image uniformity tests, as well as CT number to electron density conversion (CT-to-ED), were performed to test structural resolution and soft tissue contrast of the CBCT. This was to provide an

overview of the general image quality of the C-arm scanner and a quantitative impression whether catheter and marker identification, and CTV/OAR contouring, were possible. The details of the image quality assessments are outlined in the Data S1.

Treatment procedure

The following briefly describes the established HDR prostate brachytherapy treatment procedure at Sir Charles Gairdner Hospital (SCGH), Perth, Western Australia. The prescribed dose of 19.5 Gy is delivered over three fractions as a boost following external beam radiation therapy. The time between fractions is at least 6 h. In an operating theatre, 15–20 titanium 16 gauge afterloading catheters are inserted transperineally into the prostate under TRUS and fluoroscopy guidance. Four fiducial gold markers are also inserted transperineally into the prostate (two at the base and two at the apex of the prostate) using a biopsy needle. A silicone catheter is inserted through the urethra, and radiopaque packing is inserted into the rectum. CT images are obtained with the Toshiba Aquilion LB after the patient's recovery from anaesthesia. The SCGH HDR brachytherapy protocol is followed, that is helical scan, 2 mm slice thickness, 32 cm diameter field of view (FOV). A CTV and OARs (rectum and urethra) are contoured and fiducial markers and catheters are identified with the treatment planning system BrachyVision™ (version 10 and later version 13.7, Varian Medical Systems, Palo Alto, CA, USA). The dose is delivered with a single Ir-192 source through the titanium catheters with the GammaMedplus™ iX HDR/PDR Brachytherapy Afterloader (Varian Medical Systems, Palo Alto, CA, USA).

Study design

Six participants, who underwent HDR prostate brachytherapy in the period between May 2017 and July 2017, were recruited to the study which received approval from the SCGH Human Research Ethics Committee (Quality Improvement Approval No. 16143). In addition to the routine CT, a CBCT image (cone-beam scan, 2 mm slice thickness, 12 cm diameter (maximum) FOV) was obtained for each participant with the mobile Siemens C-arm unit when the participants were positioned on the treatment table in the HDR brachytherapy treatment room bunker prior to the first fraction. Legs were positioned the same way as for routine CT scans. The two independent image sets were separately used to plan the HDR treatment, with structures on each contoured by two radiation oncologists. Each radiation oncologist was blinded to the other's contouring and the CT and CBCT plans were generated by a different team of physicists to

avoid bias. The CT- and CBCT-based plans were spatially registered by means of rigid registration, using the implanted fiducial markers as reference points, with the software Velocity™ Advanced Imaging 3.2.0 (Varian Medical Systems, Palo Alto, CA, USA) in order to facilitate comparison, with the CBCT images resampled in the space of the CT images. Statistical analysis was undertaken with IBM SPSS Statistics 23 (IBM, Armonk, NY, USA).

CTV/OAR volumes

The volumes of the clinical structures delineated by the two radiation oncologists were calculated with Velocity™ and compared. For this, a paired samples *t*-test was conducted at 5% significance level to compare the volumes of each delineated structure in the CT and CBCT image sets.

CTV/OAR overlap

The Dice similarity coefficient (DSC)^{7,8}

$$DSC = \frac{2|X \cap Y|}{|X| + |Y|} \quad (1)$$

was calculated with Velocity™ and used to determine to what extent the CTV and the rectum of each CT- and CBCT-based plan overlap after spatial registration. *X* and *Y* are the two overlapping volumes; here CTV and OARs. Unlike the prostate, the rectum is larger in volume and extends over a longer cranial-caudal range. The radiation oncologists delineated the rectum over the same range of axial slices, that is 1–2 slices inferiorly and superiorly to the CTV. For small and narrow structures such as the urethra, the DSC is an unsuitable measure of overlap as small changes in the overlap have a large impact on the DSC which might lead to misinterpretation. Therefore, the Hausdorff distance $d_H(X, Y)$ ⁹ was used, which measures how far two objects are from each other, to assess urethra overlap

$$d_H(X, Y) = \max\{\sup_{x \in X} \inf_{y \in Y} d(x, y), \sup_{y \in Y} \inf_{x \in X} d(x, y)\} \quad (2)$$

where sup and inf are the supremum and infimum respectively.

Dose-volume histograms

Dose-volume histograms (DVH) were created for each participant for the CTV, rectum and urethra for both CT- and CBCT-based plans. Paired samples *t*-tests were

conducted at 5% significance level to compare the difference of volumes in CT- and CBCT-based plans at certain dose intervals for each clinical structure. Additionally, DVHs were created using the CBCT-planned dose distribution in combination with the spatially registered CT structures (“CT/CBCT”-based plans). Paired samples *t*-tests were again undertaken to compare the differences of volumes across DVHs created with the original CT-planned dose distribution.

Dose-volume parameters

In this study, percentage rather than absolute dose or volume is used for the subscripts *xx* in the dose-volume parameters D_{xx} and V_{xx} . The D_{xx} is the minimum dose delivered to *xx*% of the volume of the clinical structure and the V_{xx} is the volume in percentage that received *xx*% of the prescribed dose. Typical HDR prostate brachytherapy dose-volume parameters were derived (CTV: D_{90} and V_{100} , rectum: V_{80} , urethra: V_{120}) as well as values for dose constraints applied at SCGH on all CT- and CBCT-based treatment plans for comparison. Our department attempts to achieve specific constraints, that is CTV- $V_{100} = 100\%$, rectum- $V_{80} = 0\%$ and urethra- $V_{120} = 0\%$. However, these are not always achievable and each case has to be assessed individually. For the sake of better comparison, tolerances in this study were set uniformly for all participants, that is CTV- $V_{100} > 90\%$, rectum- $V_{80} < 2\%$ and urethra- $V_{120} < 2\%$. Paired samples *t*-tests were conducted at 5% significance level to compare the differences of dose-volume parameters in CT- and CBCT-based treatment plans.

Results

Image quality assessments

The 10%-MTF (modulation transfer function) of the Siemens CBCT was 7.2 ± 1.0 . Applying the Nyquist theorem on the 10%-MTF revealed that structures with length *L* of 0.69 mm were still spatially resolvable. The uniformity tests on the Siemens CBCT revealed capping artefacts and a steep gradient in CT numbers at the edge of the FOV. The CT-to-ED conversion showed that the CBCT underestimated the absolute CT numbers of all tissue and bone types. See Data S1 for more details.

Study design

The mean age of participants was 73.80 years, standard deviation (SD) 7.46 years. Figure 1 depicts the axial CT image and the corresponding CBCT image of participant 05 (a, b) and of participant 03 (c, d) showing the

catheters and two of the fiducial markers. Compared to CT, the FOV in the CBCT images was smaller, more streaking artefacts were present, and the soft tissue contrast was lower. One of the six CBCT sets was considered unsuitable for treatment planning as some of the catheters were located beyond the boundary of the FOV due to non-ideal positioning of the C-arm gantry. As such, results below are for five participants only. Figures 2 and 3 show the axial view (left), sagittal view (top right) and coronal view (bottom right) of the spatially registered CT and CBCT image sets of participant 05 and 03 respectively. The CT images are coloured in grey and the CBCT in yellow. The axial plane is the same as in Figure 1 and the three planes (axial, sagittal, coronal) are focussing the same fiducial marker (red circled cross). The green contours are the CTV delineation of each image set overlapped.

CTV/OAR volumes

Table 1 shows the results of the *t*-tests comparing the volumes of each delineated structure in the CT and CBCT image sets. The mean differences indicated larger

CTVs and urethrae, and smaller rectums were contoured on the CBCT relative to CT images. However, for the CTV ($P = 0.087$), rectum ($P = 0.262$) and urethra

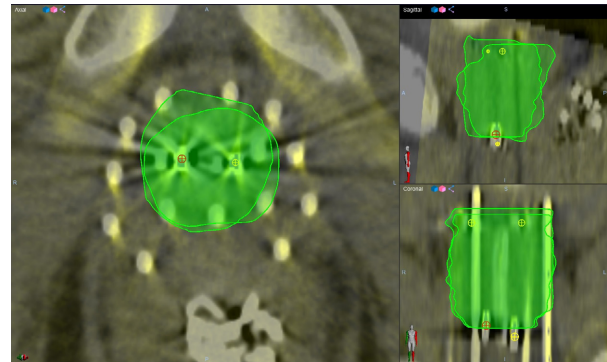


Figure 2. Axial view (left), sagittal view (top right) and coronal view (bottom right) of spatially registered CT (grey) and CBCT (yellow) image set of participant 05 showing example contours of a high CTV overlap (DSC = 0.85). The three planes are focussing the same fiducial marker (red circled cross). The axial plane is the same as in Figure 1a, b.

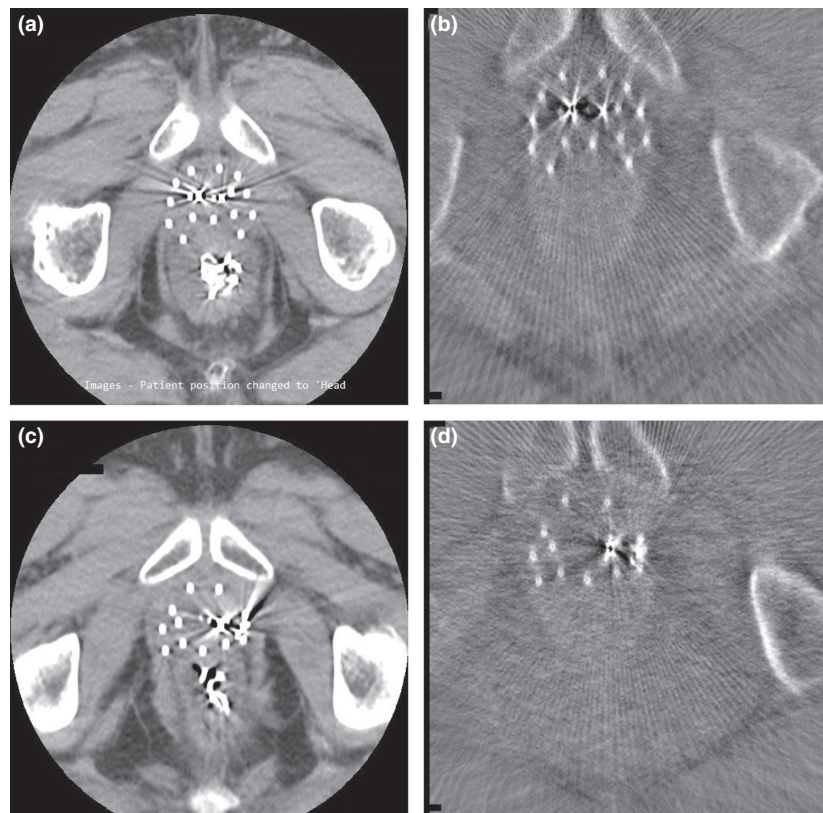


Figure 1. Sample CT image (a) and corresponding CBCT image (b) of participant 05. Sample CT image (c) and corresponding CBCT image (d) of participant 03.

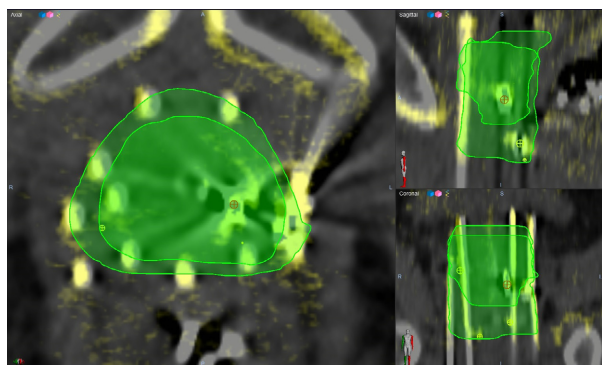


Figure 3. Axial view (left), sagittal view (top right) and coronal view (bottom right) of spatially registered CT (grey) and CBCT (yellow) image set of participant 03 showing example contours of a low CTV overlap (DSC = 0.63). The three planes are focussing the same fiducial marker (red circled cross). The axial plane is the same as in Figure 1c, d.

Table 1. Results of the paired samples *t*-tests to compare the volumes of each delineated structure in the CT and CBCT image sets where CI is the confidence interval. The units are in cm³.

	Mean (CT)	Mean (CBCT)	Mean difference	95% CI lower	95% CI upper	<i>P</i> -value
CTV	28.5	33.5	-5.0	-11.2	1.2	0.087
Rectum	83.1	52.3	30.9	-34.8	96.5	0.262
Urethra	1.3	1.5	-0.2	-0.4	0.0	0.088

(*P* = 0.088), the results suggested that there was no statistically significant difference between the volumes.

CTV/OAR overlap

Figure 4 shows a box plot including the raw data points for each clinical structure where the DSC on the left axis is referring to the CTV and rectum, and the Hausdorff distance on the right to the urethra. The mean DSC and SD for the CTV and rectum were 0.73 ± 0.08 and 0.63 ± 0.06, respectively, which were according to Velker et al.¹⁰ a moderate level of agreement between delineated volumes, that is mean DSC 0.60–0.79. The mean Hausdorff distance and SD for the urethra was 5.72 ± 2.08 mm. Figures 2 and 3 show an example of a high (0.85) and a low (0.63) DSC.

Dose-volume histograms

Figure 5 shows the DVHs of all five participants generated with the built-in optimiser of the treatment planning system. The green, dark-blue and cyan graphs are the dose-volume data points of the CTV, urethra and

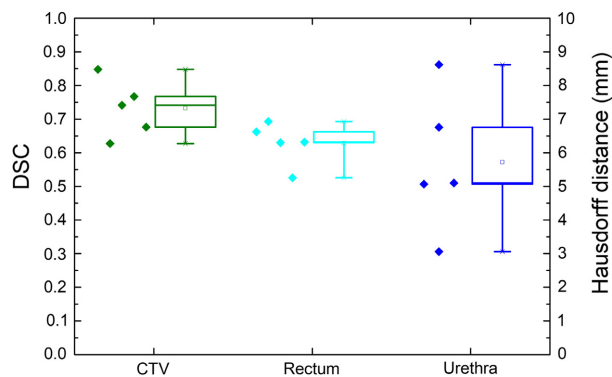


Figure 4. Box plots including raw data points for each clinical structure where the DSC on the left axis is referring to the CTV and rectum, and the Hausdorff distance on the right to the urethra. Whiskers show minimum and maximum value; boxes, the interquartile range; horizontal lines, the median and squares the mean.

rectum respectively. The solid lines represent the data from the CT-based treatment plans, the dashed lines from the CBCT-based plans and the dotted lines from the CT/CBCT-based plans.

Figure 6 shows the results of the paired *t*-tests comparing the difference of volumes both in CT and CBCT, as well as in CT- and CT/CBCT-based treatment plans at certain dose intervals for each clinical structure. The horizontal line represents the 5% significance level and the vertical line the prescribed dose of 19.5 Gy. In both comparisons, for the CTV there was a statistical significant difference evident for dose intervals beyond the prescribed dose, and for the urethra for one single dose interval. In the CT and CBCT comparison, for the rectum there were several dose intervals where the *P*-value was below the threshold.

Dose-volume parameters

Figure 7 shows box plots of various dose-volume parameters calculated from CT-, CBCT- and CT/CBCT-based treatment plans. Table 2 shows the results of the paired samples *t*-tests comparing the CT and CBCT plans. Apart from one participant, CTV-*D*₉₀ was above the prescribed dose of 19.5 Gy and CTV-*V*₁₀₀ was greater than 91%. Values for rectum-*V*₈₀ and urethra-*V*₁₂₀ were less than 0.3% and 1.6% respectively, for all treatment plans.

Table 3 shows the results of the paired samples *t*-test comparing the CT- and CT/CBCT-based treatment plans. Apart from the one participant mentioned before, there was another participant’s plan that failed to achieve sufficient CTV coverage, that is CTV-*D*₉₀ = 17.1 Gy and CTV-*V*₁₀₀ = 81.7%. Values for rectum-*V*₈₀ and urethra-*V*₁₂₀ were

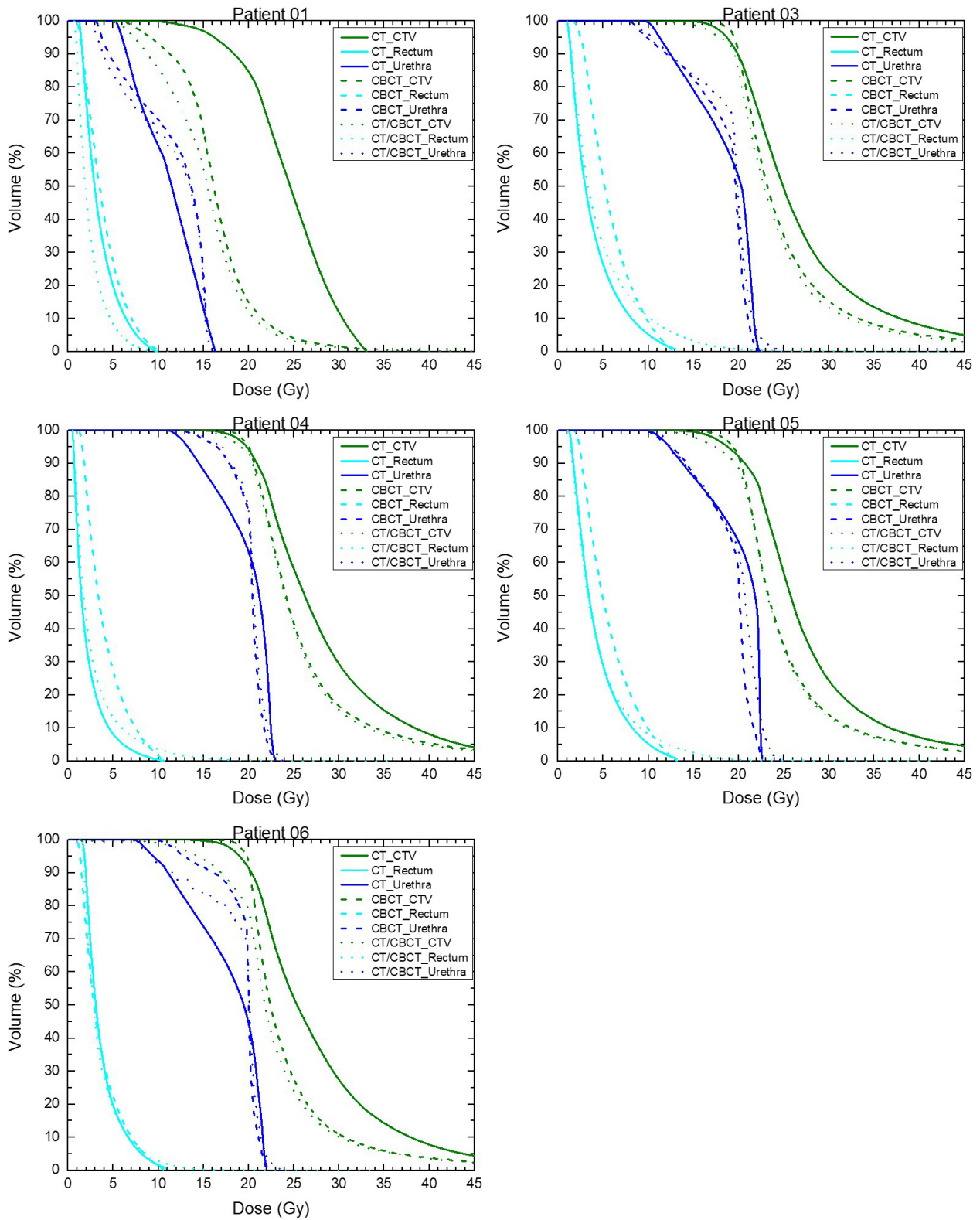


Figure 5. Dose-volume histograms of all participants: Solid, dashed and dotted lines represent the CT-, CBCT- and CT/CBCT-based treatment plans respectively. Green, blue, cyan are the CTV, urethra and rectum respectively.

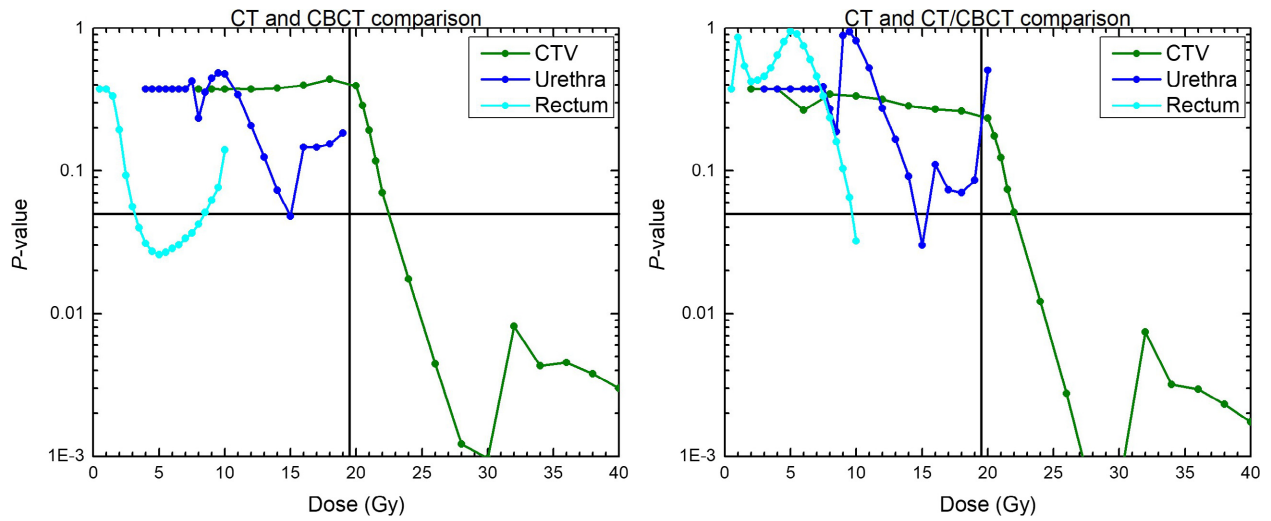


Figure 6. The results of the paired samples t-tests comparing the difference of volumes in CT- and CBCT-based treatment plans (left) and in CT- and CT/CBCT-based plans (right). The p-values are logarithmically plotted against various dose intervals.

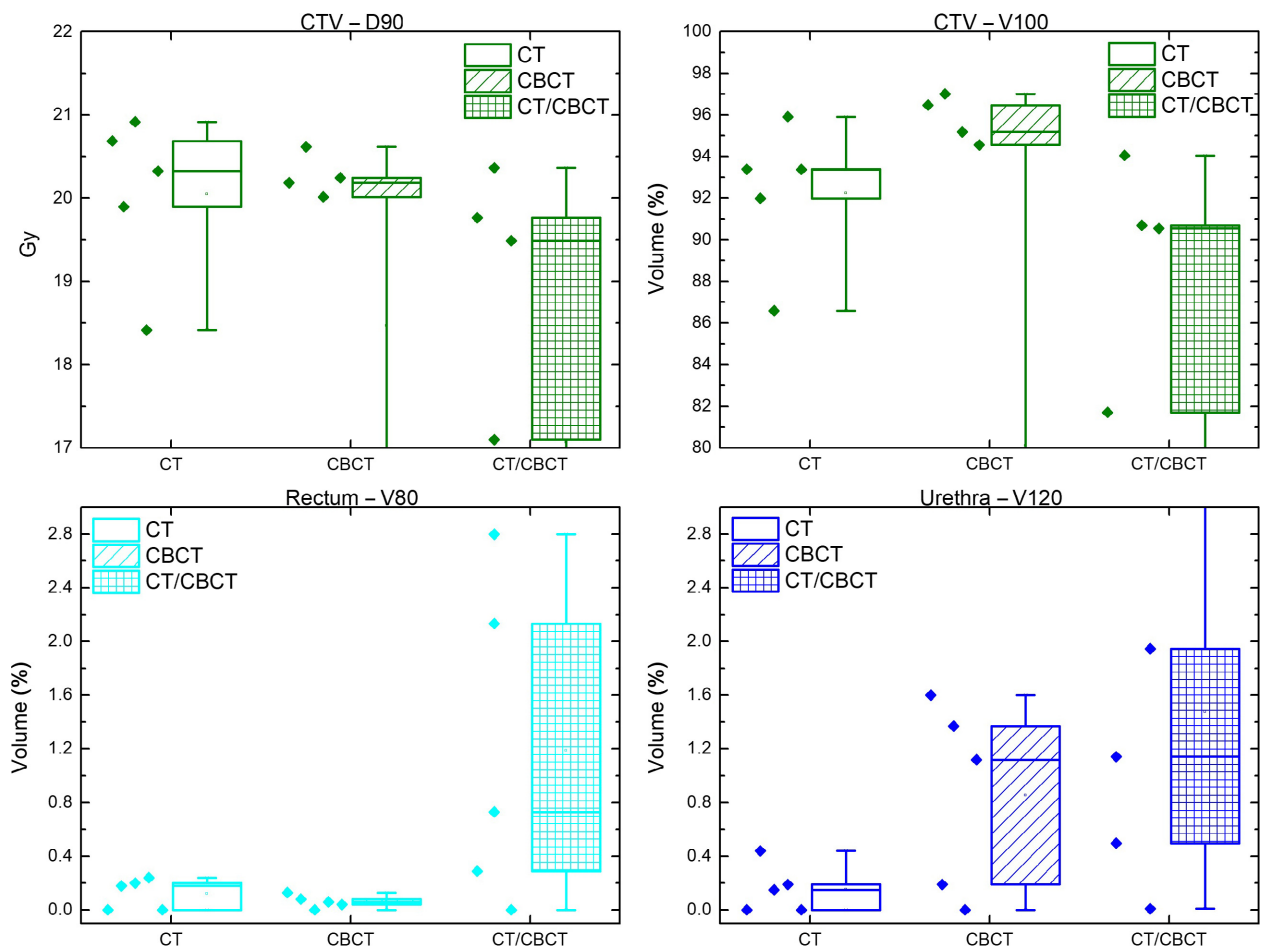


Figure 7. Various dose-volume parameters comparing CT-, CBCT- and CT/CBCT-based treatment plans: CTV-D₉₀, CTV-V₁₀₀, rectum-V₈₀, and urethra-V₁₂₀.

Table 2. Results of the paired samples *t*-tests comparing the difference of dose constraints in CT- and CBCT-based treatment plans.

	Mean (CT)	Mean (CBCT)	Mean difference	95% CI lower	95% CI upper	<i>P</i> -value
CTV D_{90} [Gy]	20.1	18.5	1.6	-2.3	5.4	0.320
CTV V_{100} [%]	92.3	80.1	12.1	-27.5	51.8	0.443
Rectum V_{80} [%]	0.1	0.1	0.1	-0.1	0.2	0.387
Urethra V_{120} [%]	0.2	0.9	-0.7	-1.8	0.4	0.137

Table 3. Results of the paired samples *t*-tests comparing the difference of dose constraints in CT- and CT/CBCT-based treatment plans.

	Mean (CT)	Mean (CT/CBCT)	Mean difference	95% CI lower	95% CI upper	<i>P</i> -value
CTV D_{90} [Gy]	20.1	17.1	3.0	-2.0	7.9	0.169
CTV V_{100} [%]	92.3	74.2	18.1	-20.2	56.3	0.260
Rectum V_{80} [%]	0.1	1.2	-1.1	-2.6	0.5	0.125
Urethra V_{120} [%]	0.2	1.5	-1.3	-3.2	0.6	0.121

less than 2.8% and 3.8% respectively, for all treatment plans.

The results of the *t*-tests suggest that there were no statistically significant differences between CT and CBCT for all dose-volume parameters. This was also the fact when comparing CT- and CT/CBCT-based treatment plans since all *p*-values were greater than 0.05. It has to be noted, however, that the sample size in this study was very small which makes it harder to find statistical significance. The magnitude of the differences in CTV- V_{100} was, however, of clinical significance.

Discussion

Image quality assessments and identification of catheters and markers

Figure 1 indicates that catheters and fiducial markers were visible and distinguishable which was in accordance with the spatial resolution test, that is structures with a length of 0.69 mm were still spatially resolvable (see Data

S1). The catheters used were 1.8 mm in diameter and the fiducial markers were 5 mm in length and 1.0 mm in diameter. Moreover, Figures 2 and 3 show that catheters and markers were also visible in the sagittal and coronal plane and that they overlapped with the CT ones, that is yellow on grey.

There were some challenges during the process. Although the catheters were spatially distinguishable, the auto catheter path detection algorithm in the treatment planning system, which attempted to automatically trace the catheter paths based on CT number differences between the actual catheter and the proximal ambience, was less accurate in the CBCT images due to streaking artefacts in these images. Reconstruction involved more manual adjustments to identify the catheter paths which prolonged the process. The image quality of the catheter tips was slightly poorer in the CBCT images. Although this did not hinder the identification process, it resulted in prolonging the process. There were no challenges during the identification of the fiducial markers. Ultimately, the image quality of the catheters and markers was sufficient for identification in the planning process. The inconvenience of additional time required for the process was not significant considering the overall time for treatment planning.

However, there was potential for acquiring an image that was unsuitable for planning due to the small FOV of the Siemens CBCT and its impact as determined from the uniformity test. The effective size of the FOV determined with our proposed method was on average 10.6 cm rather than 12 cm (see Data S1). The clearance diameter between the X-ray tube and the image intensifier was 80 cm. One study participant was excluded as the catheters on the participant's CBCT images were distorted at the boundary of the FOV which made catheter identification impossible. In this case, the combination of the participant's high body mass index, the effective FOV, the clearance diameter of the C-arm gantry, and the width and thickness of the treatment table (60 and 10 cm) hampered the positioning of the prostate into the isocentre which led to the unsuccessful catheter identification.

Generally, imaging the region of interest in the isocentre is not always possible since the C-arm gantry might collide with either the patient or the treatment table depending on the patient size. Therefore, the anatomy of the patient limits the use of the Siemens CBCT and is not suitable for all patients. It is also necessary to ensure that the catheters and prostate are scanned in a region with high uniformity to obtain the possibly best treatment plan in HDR prostate brachytherapy since deteriorated uniformity affects soft tissue contrast and ultimately CTV/OAR contouring accuracy.

CTV/OAR volumes and overlap

For the CTV, the mean difference of the relative volume was lower and the DSC was higher compared to the rectum. The differences in volumes and the moderate level of agreement of the DSC were attributed to both different modalities and observers. Since the CT and CBCT image sets were contoured by different radiation oncologists, it was not clear whether the modality or observer contributed to the differences. However, since there was no statistically significant difference in volumes and the observers had a moderately good level of agreement with regard to the CTV/OAR overlap, there was an indication that the differences were more likely attributed to the different modalities. The determined differences were of the order found in previous studies identifying differences in CT-derived prostate volumes by pairs of observers.¹¹ The radiation oncologists reported that they were able to use the fiducial markers and catheters as a contouring aid. In all plans, the overlapped urethra crossed in the centre of the prostate in form of an "X". Therefore, Hausdorff distances were determined either superiorly to the base or inferiorly to the apex of the prostate. Both radiation oncologists agreed anecdotally that the contouring was more challenging on the CBCT images which was confirmed in the CT-to-ED conversion (see Data S1). The C-arm CBCT underestimated the absolute CT numbers for all tissue types relative to the Toshiba CT-derived values. The spectrum of CT numbers ranging from air to bones in CBCT was shorter compared to CT varying from approximately -200 to 700 HU (-1000 to 2000 HU in CT). This reduced the already limited CT number range of soft tissue which could exacerbate recognised difficulties in contouring of the CTV and surrounding OARs. Moreover, typical cone-beam-associated issues such as increased scatter and noise, beam hardening, decreased contrast, streak and truncation artefact alter the CT numbers.¹² Increased scatter lowers the apparent CT number as more scattered photons are detected.

Dose-volume histograms

For Figure 5, the DVHs for CBCT and CT/CBCT were similar. This suggests that coverage of the original CT-derived structures using the CBCT-derived dose was much the same as coverage of the CBCT-derived structures with that dose. However, the coverage of the CT-derived structures with the CT-derived dose was quite different mainly for the CTV and at very high doses well above the prescription where they were statistically significantly higher in Figure 6. This might be due to small catheter position changes which led to higher dose changes. With the CT CTV volumes smaller than the CBCT CTV volumes (Table 1), these high-dose regions

covered proportionally more of the CT CTV and hence, the relative DVHs were higher in that region.

The region of statistical significant difference in rectal DVHs in Figure 6 reflected a tendency for reduced dose to the rectum in the CT-based plan. This could be due to both the smaller CT CTVs, which kept high-to-medium isodoses in the steep gradient covering a smaller portion of the anterior rectum for the CT-based plans, as well as the smaller rectum on CBCT closer to the larger volumed CTVs, meaning mid-to-higher doses covered proportionally more of the rectum in the CBCT plans.

Dose-volume parameters

All CT and CBCT treatment plans passed the rectum and urethra dose constraints. The CTV constraints were passed by all but one single participant. At this stage, it was not clear why the CTV constraints failed in both CT and CBCT plan for this particular participant. There are two participants who failed both the rectum and urethra dose constraints in the CT/CBCT treatment plans. Another participant failed the CTV coverage on the CT/CBCT plan. The paired samples *t*-tests suggested that there is no statistical significant difference between CT and CBCT, as well as CT- and CT/CBCT-based treatment plans. However, the mean difference of the CTV- V_{100} between the CT and CBCT, and CT and CT/CBCT plans are 12.13% and 18.07%, respectively, which would be unacceptable in clinical practice.

Recommendations for a suitable mobile C-arm CBCT unit

The study showed that the Siemens Arcadis Orbic 3D was feasible for catheter and fiducial marker identification but had its limitations in the use for CTV and OARs contouring. However, the presented treatment plan comparisons indicated that the CBCT plans were comparable to the CT plans meaning that standard quality CT images may not be necessary for HDR prostate brachytherapy treatment planning. The following recommendations from the authors were based on the observations obtained during this study. A suitable CBCT unit for HDR prostate brachytherapy treatment planning should have a similar spatial resolution as the unit used in this study but with a superior low-contrast resolution in order to have a higher certainty in CTV and OAR contouring, that is the spectrum of CT numbers from air to bones should be longer than the current one ranging from approximately -200 to 700 HU (see Data S1). To facilitate the positioning of the prostate at isocentre and to avoid collision, this work suggests that the suitable C-arm CBCT unit has a FOV at least 5 cm larger than the tested Siemens unit, and a flat panel detector rather

than an immense image intensifier. The treatment table in theatres should ideally be as narrow as possible.

Conclusion

Despite the fact that the catheters and fiducial markers were indeed identifiable and localisable in the CBCT images and the potential benefits of using mobile CBCT over CT, the study concludes that the particular unit tested, the Siemens Arcadis Orbic 3D, cannot feasibly and solely be used for HDR prostate brachytherapy treatment planning without any other aiding imaging modality such as TRUS. The image quality assessments revealed, and the radiation oncologists confirmed, that particularly the contouring is more challenging and the weakest link of the treatment planning chain due to low soft tissue contrast. Moreover, imaging the region of interest in the isocentre was not always possible since the C-arm gantry might collide with either the patient or the treatment table depending on the patient size. Therefore, the anatomy of the patient limits the use of the tested Siemens CBCT unit and is thus not suitable for all patients. However, it is noteworthy that statistically speaking (small sample size notwithstanding) the CBCT plans were comparable to the CT plans based on DVHs and dose-volume parameters, despite higher uncertainties in delineating the CTV and OARs on the CBCT due to poorer image quality. This indicates that standard quality CT images may not be necessary for HDR prostate brachytherapy treatment planning. This shows that another model of mobile CT scanner with sufficient soft tissue contrast that provides a higher certainty in contouring CTV and OARs could be feasible for HDR prostate brachytherapy treatment planning and the methods outlined in this study could be used for evaluation.

Acknowledgements

The authors thank the departments of Radiation Oncology and Medical Technology & Physics of Sir Charles Gairdner Hospital in Perth, particularly Mahsheed Sabet, Godfrey Mukwada, Zaid Alkhatib and Rikki Nezich, for the support, the fruitful discussions and the provision of equipment used for this presented work.

Conflict of Interest

The authors declare no conflict of interest.

References

1. Scarfe WC, Farman AG. What is cone-beam CT and how does it work? *Dent Clin North Am* 2008; **52**: 707–30.
2. Al-Halabi H, Portelance L, Duclos M, Reniers B, Bahoric B, Souhami L. Cone beam CT-based three-dimensional

- planning in high-dose-rate brachytherapy for cervical cancer. *Int J Radiat Oncol Biol Phys* 2010; **77**: 1092–7.
3. Holly R, Morton GC, Sankrecha R, et al. Use of cone-beam imaging to correct for catheter displacement in high dose-rate prostate brachytherapy. *Brachytherapy* 2011; **10**: 299–305.
4. Herrmann MK, Kertesz T, Gsanger T, et al. Gold marker displacement due to needle insertion during HDR-brachytherapy for treatment of prostate cancer: A prospective cone beam computed tomography and kilovoltage on-board imaging (kV-OBI) study. *Radiat Oncol* 2012; **7**: 24.
5. Batchelar D, Gaztañaga M, Schmid M, Araujo C, Bachand F, Crook J. Validation study of ultrasound-based high-dose-rate prostate brachytherapy planning compared with CT-based planning. *Brachytherapy* 2014; **13**: 75–9.
6. Even AJG, Nuver TT, Westendorp H, Hoekstra CJ, Slump CH, Minken AW. High-dose-rate prostate brachytherapy based on registered transrectal ultrasound and in-room cone-beam CT images. *Brachytherapy* 2014; **13**: 128–36.
7. Dice LR. Measures of the amount of ecologic association between species. *Ecology* 1945; **26**: 297–302.
8. Sørensen T. A method of establishing groups of equal amplitude in plant sociology based on similarity of species and its application to analyses of the vegetation on Danish commons. *Biol Skr* 1948; **5**: 1–34.
9. Huttenlocher DP, Klanderman GA, Rucklidge WJ. Comparing images using the Hausdorff distance. *IEEE Trans Pattern Anal Mach Intell* 1993; **15**: 850–63.
10. Velker VM, Rodrigues GB, Dinniwel R, Hwee J, Louie AV. Creation of RTOG compliant patient CT-atlases for automated atlas based contouring of local regional breast and high-risk prostate cancers. *Radiat Oncol* 2013; **8**: 188.
11. Dubois DF, Prestidge BR, Hotchkiss LA, Prete JJ, Bice WS. Intraobserver and interobserver variability of MR imaging- and CT-derived prostate volumes after transperineal interstitial permanent prostate brachytherapy. *Radiology* 1998; **207**: 785–9.
12. García-Vázquez V, Marinetto E, Guerra P, et al. Assessment of intraoperative 3D imaging alternatives for IOERT dose estimation. *Z Med Phys* 2017; **27**: 218–31.

Supporting Information

Additional supporting information may be found online in the Supporting Information section at the end of the article.

Data S1. Methods, results and discussion of image quality assessments (spatial resolution, image uniformity, and CT to electron density conversion) conducted on the Siemens Arcadis Orbic 3D mobile C-arm CBCT.